Substituting fossil-based with bio-based chemicals: The case of limonene as a greener pore expander for micellar templated silica

Umair Sultan, Katrin Städtke, Andreas Göpfert, Daniel Lemmen, Ezzeldin Metwali, Santanu Maiti, Carola Schlumberger, Tadahiro Yokosawa, Benjamin Apeleo Zubiri, Erdmann Spiecker, Nicolas Vogel, Tobias Unruh, Matthias Thommes, Alexandra Inayat*

affiliation of all authors: Friedrich-Alexander University Erlangen-Nürnberg, Erlangen, Germany

*corresponding email address: alexandra.inayat@fau.de

Abstract

Porous materials are widely used in applications such as adsorption, catalysis and separation. The use of expander molecules is a versatile route to enlarge the mesopore size in micellar templated mesoporous silica materials. Typical expanders used for this purpose are fossil-based organic molecules such as trimethylbenzene (TMB). In the course of making such syntheses greener and more sustainable, it is highly desirable to substitute such fossil-based chemicals with renewable ones. Here, we show that bio-based limonene can be used as an alternative expander molecule for the synthesis of large-pore templated silica. On the basis of electron microscopy, nitrogen physisorption and small angle X-ray scattering we show that the substitution of TMB by limonene leads to very similar material characteristics, reaching mean mesopore diameters of 17-19 nm. A comparative life-cycle assessment demonstrates the reduced environmental impact of limonene production from citrus peel waste compared to TMB production, supporting the call for more applications of renewable chemicals, ideally from waste-streams, also for the production of porous materials.

Introduction

The development of greener synthesis approaches is a vital element of making chemicals and materials production more sustainable e.g., by reducing harmful emissions, stopping the depletion of non-renewable raw materials and integrating anthropogenic production processes into natural materials cycles.[1,2]

Porous materials are a huge group of materials occurring directly or indirectly in our daily life, from washing powder, thickeners in paints, auxiliaries in pharmaceutical production, car exhaust gas catalysts up to the little silica gel sachets we often find in new shoes and electronic equipment to control humidity. Among these, micellar templated silica (MTS, often also named as ordered mesoporous silica) constitutes a large class of mesoporous materials with amorphous silica walls surrounding a defined mesopore system.[3] MTS materials have wide-spread industrial and potential applications as catalyst support[4] e.g. for enzymes,[5,6] Keggin ions,[7] and for biorefinery-related conversions,[8] chromatography column material and metal extraction,[3] drug delivery matrix,[9] gas adsorption and storage,[10] and many other processes requiring large interfaces and pore volumes accessible also for larger (e.g. bio-based) molecules. Their synthesis requires a silica source, a solvent (typically water), acids or bases to adjust the pH, and organic substances to template and tailor the defined mesopore system for their specific applications.[3]

The pore diameter of MTS materials like SBA-15 (cylindrical mesopores) is typically in the range of 5-10 nm, under certain synthesis conditions even 15 nm.[11] With the help of expander molecules (swelling agents) this pore diameter can be increased by several nanometres as illustrated in Figure 1. If the expander amount exceeds a certain expander to mesopore template ratio then the well-ordered pore alignment (e.g. hexagonal in the case of SBA-15) is lost and can transform towards spherical MCF pore structure with cell sizes in the range of 22-42 nm and pore entrances of 8-23 nm.[12,13]

The prevalent expander molecule for MTS syntheses, in the presence of cationic[14] and also neutral surfactants like poloxamers (e.g. Pluronic P123), is trimethyl benzene.[13] Also, n-octane,[15] toluene,[16,17] xylenes, ethylbenzene, toluene, cyclohexane and 1,3,5-triisopropyl benzene[7,18,19] have been reported for pore expansion.

Many of the substances involved in MTS synthesis are yet fossil-based, corrosive or even hazardous, but greening efforts are already underway and emerge as a growing research direction in porous materials preparation.[20] For example, the phospholipide lecithin,[21] alkylglycosides,[22,23] palmitic acid,[24] tannic acid,[25] oleylamines,[26] gelatine,[27] and yeast-derived sophorolipids[28] were successfully applied as bio-based mesopore templates. Some of these templates such as tannic acid and gelatine were reported to also increase the pore size of the obtained materials. In another greening approach, the use of strong acids (typically HCl) and post-synthetic neutralisation washes in SBA-15 synthesis were avoided by a novel UV-light based radical method to control silica condensation.[29]

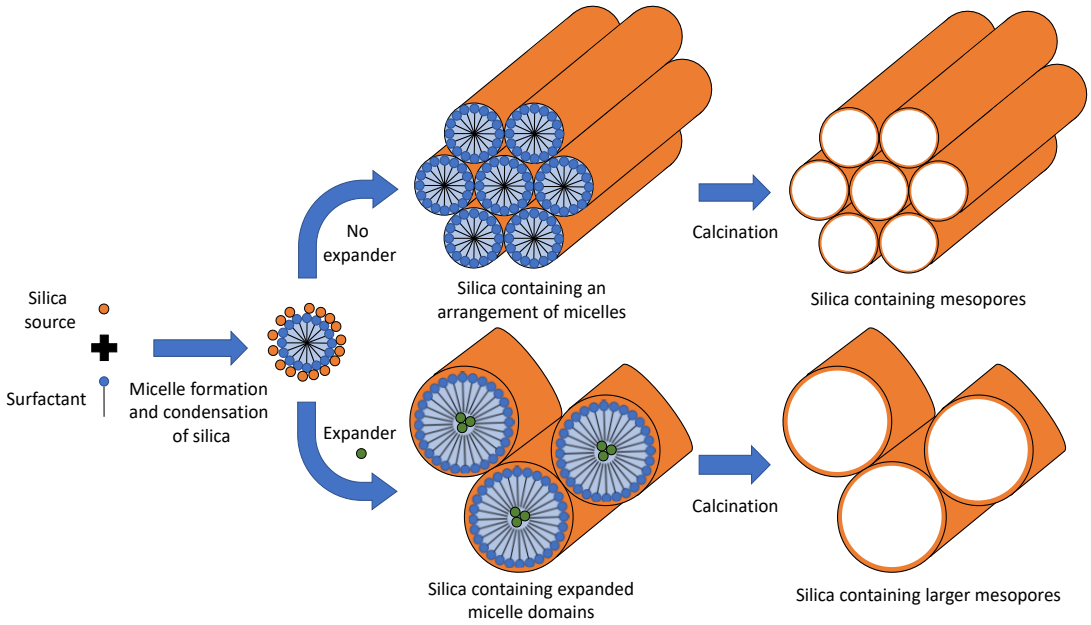

Figure 1. Schematic illustration of the expander action in micellar templated silica

Another but yet unexplored approach for greener MTS synthesis is the substitution of the above-mentioned, all fossil-based expander molecules (micelle swelling agents) by bio-based i.e., renewable ones. Accordingly, this contribution extends the choice of renewable expander molecules and presents a study on substituting the conventional fossil-based expander molecule TMB with the bio-based molecule limonene. Limonene is a cyclic monoterpene (Figure 2) with lemon-like smell, yellow colour and wide use e.g. as bio-based solvent and fragrance in commodities like shower gel and soap.[30] With 95 % it is the main constituent of citrus peel oil[31] but is also present in turpentine oil and can be obtained via isomerisation of pinene, which is the main constituent of turpentine oil (a by-product of the wood and paper industry).[32] Accordingly, limonene is currently mainly produced from upcycled waste streams of the food and paper industry, making its use very desirable in respect to a more efficient raw material consumption and waste prevention,[1] which is in line with the 12th UN Sustainable Development Goal (Responsible Consumption and Production). Limonene does not belong to the group of substances of very high concern,[33] which is an important precondition for the exploitation of any chemical towards more sustainable production processes.[34] From a materials synthesis point of view, we found limonene interesting as bio-based alternative to TMB and other aromatic/cyclic expander molecules in MTS synthesis because it has a comparable composition and molecular structure (Figure 2) and would therefore potentially

interact in a similar manner with the mesopore template Pluronic P123 (polyethylene polypropylene triblock copolymer).

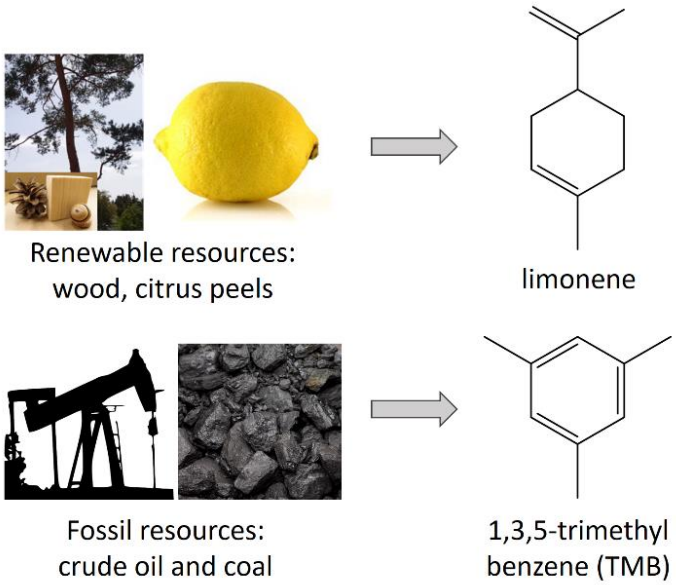

Figure 2. Current raw materials and molecular structure of TMB and limonene which were investigated as expander molecules for micellar templated silica in the present study.

In the second part of this contribution the results of the life cycle assessment are presented, which we conducted in order to clarify if the substitution of TMB by limonene is not only greener by fulfilling one of the twelve green chemistry principles (i.e., use of renewable materials)[35] but more importantly if it has also less environmental impacts considering the whole production chain from raw materials sourcing up to expander production.

Results and discussion

Comparative characterisation of mesoporous silica obtained using different amounts of limonene and TMB as expander

To compare the pore expanding effect of limonene and TMB we conducted silica syntheses with increasing amounts of both expander molecules using the triblock co-polymer Pluronic P123 as templating agent. The textural data of the resulting materials (pore size distribution, pore volume, specific surface area) were determined from nitrogen physisorption isotherms which are shown in Figure 3a and 3c. All isotherms are of type IVa,[36] indicating the presence of mesopores in the material. An increase in total adsorbed volume is observed as the amount of added expander is increased. The total adsorbed volume is an indication for the volume of mesopores inside the material. As can be seen from Table 1, similar amounts of TMB and limonene, respectively, lead to similar total pore volume. Furthermore, an increasing expander amount results in a shift of the hysteresis loop in the isotherms to higher relative pressure values, which indicates an increase of the average pore size. This increase is also visible in the pore size distribution curves (Figures 3b, 3d). Moreover, for all samples the adsorption and desorption branches of each isotherm (Figures 3a and 3c) run parallel to each other and with narrow distance resulting in a H1 hysteresis.[36] Such shape of the hysteresis loop in the isotherms indicates that the pore morphology is predominantly cylindrical with the majority of pores being freely accessible and not restricted by narrower pore windows.[37,38] This is also indicated by the good agreement of the pore size distributions determined from the adsorption branch using a cylindrical

metastable NLDFT adsorption branch kernel with the pore size distributions calculated from the desorption branch using a cylindrical equilibrium NLDFT kernel (Figure S1).

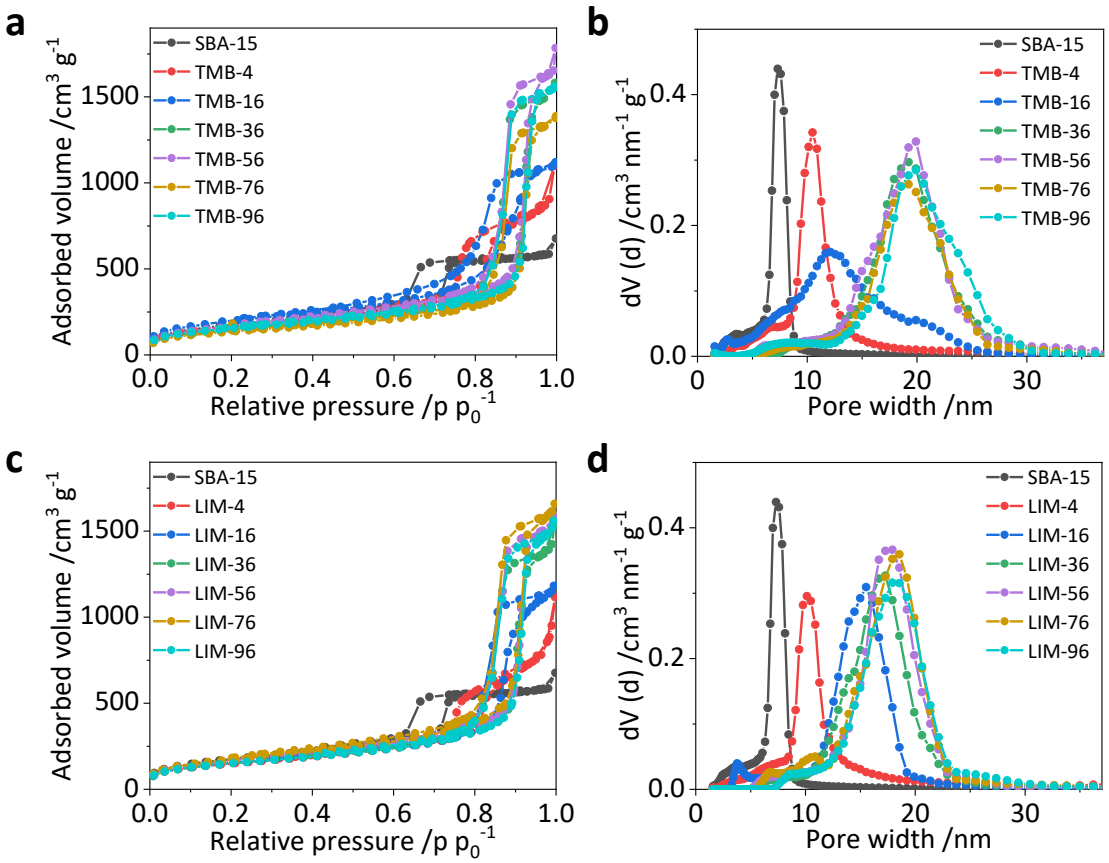

Figure 1. N_2 physisorption data for varying amounts of TMB (top row) and limonene (LIM, bottom row) expander. The isotherms for samples synthesized using (a) TMB and (c) limonene, are all of type IVa. The pore size distributions in (b) and (d) show a gradual increase in pore size with increasing expander to P123 molar ratio.

This interpretation is also supported by the TEM images in Figure 4, where we see that syntheses without and with small amounts of expander lead to ordered cylindrical pores. Increasing the expander to P123 molar ratio towards 36 results in a loss of the regular alignment of the pore openings (Table 1) without indication for spherical (foam-like) pores. As the expander amount increases the maxima of the pore size distribution curves shift progressively from 7.5 nm for SBA-15 (Figure 3b and 3d, black curve) to ~19 and ~17 nm for TMB-36 and LIM-36 (Figure 3b and 3d, green curve). Further increase in expander amount does not result in further increase of the pore sizes, indicating that the maximum expansion of the pores has been achieved at a ratio of 36 for both the expanders. Textural data for all the samples are listed in Table 1. These results clearly demonstrate the pore expanding capabilities of limonene and show that it is very similar to TMB.

In addition to the pore size, the expander amount also has a major influence on the pore morphology and arrangement which was visualized through transmission electron microscopy (TEM) analysis (Figure 4). In the sample synthesised without expander (Figure 4a) we observe hexagonally arranged cylindrical pores which are characteristic for SBA-15.[12] The addition of small amounts of expander TMB and limonene, respectively, widens the pore space and still results in long channel-like pores that run parallel along the entire particle (Figure 4b and 4e). But in contrast to the reference sample (SBA-15) these channels twist and turn at different angles, which correlates with the changed morphology of the porous particles (SEM images in Figures 5b and 5i). Further increase of the amount of both expanders leads to progressive loss of the ordered arrangement of the pores. In the case of TMB

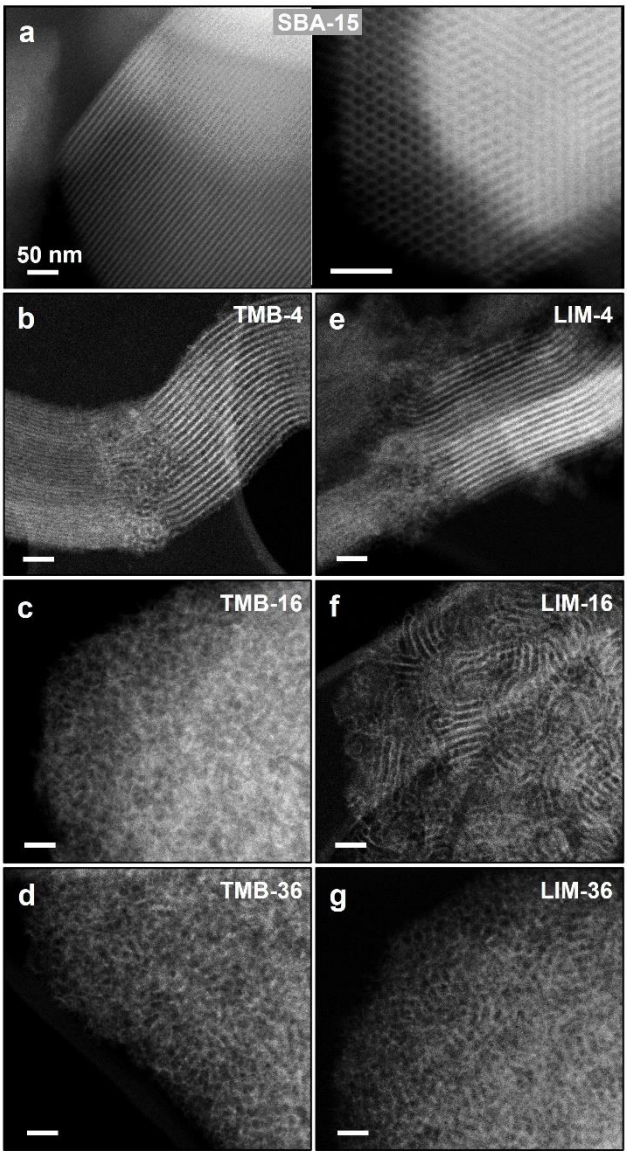

Figure 4. TEM images for mesoporous silica synthesized with increasing expander/P123 molar ratios from 4 up to 36 for both TMB (left column) and limonene (right column). As a reference the SBA-15 sample synthesised in the absence of expander molecules is depicted in the upper image (a) showing the cylindrical pores in side-view (left) and viewed along the pore channels (right). The scale bar for all images is 50 nm.

this structural loss is already pronounced for an expander/P123 molar ratio of 16 (Figure 4c) and in the case of limonene at an expander/P123 ratio of 36 (Figure 4g). Accordingly, at an expander/P123 ratio of 36, a similar pore morphology is obtained for both expander molecules with no further increase of pore size, pore volume and surface area as seen from the nitrogen physisorption results (Table 1).

Scanning electron microscopy (SEM) was used to compare the influence of both expander molecules on the particle morphology (Figure 5, Figure S2). For the sample with no expander, we see a faceted morphology that has been previously observed for SBA-15 materials.[39] With the addition of small expander amounts (TMB-4 and LIM-4), the particles transform into long agglomerated strands (Figure 5b and 5h). As observed in the TEM images, these strands contain long twisted channels running parallel through the entire particle (Figure 4b and 4e). When the expander amount is further increased (expander/P123 ratios of and above 16), the particles show a spherical agglomerated morphology (Figures 5c-g and 5i-m) which is similar for both, TMB and limonene. Here, the expanded pore entrances are already visible at the particle surface.

The pore structure of the samples was further examined using small angle X-ray scattering (SAXS) technique (Figure 6). The 1D SAXS profile of the reference sample (SBA-15) shows several strong scattering peaks (Figure 6, blue line) whose positions have a relative ratio of 1 : √3 : √4 : √7. This corresponds to a well-ordered hexagonally close-packed (HCP) superstructure[40] which is expected for SBA-15.[41] The extracted lattice parameter is 11.1 nm, representing the pore centre–centre distance of HCP cylindrical pores in the sample. Together with the TEM-based pore wall thickness of 3.3 nm the calculated pore diameter of 7.8 nm agrees well with the results from nitrogen physisorption (7.5 nm). For the sample with low ratio of expander/P123 (LIM-4), the HCP pore structure persists, however the lattice parameter increased to 12.7 nm. When the amount of limonene was further increased, (LIM-16) a transition from HCP to a less ordered structure at a repeating distance of 13.3 nm is observed with scattering peaks at ratios of 1: 2: 3.

For further increase in expander amount (LIM-36, LIM-56, LIM-76), the scattering profiles show peak broadening which suggests that the pore arrangement becomes less ordered with a periodic distance of 18.4-19.6 nm. For the TMB samples quite similar results as for the limonene samples are found. For the sample with low amount of expander (TMB-4), the scattering peaks have an intermediate peak position ratio, which corresponds to a distorted HCP or body centered rectangular superlattice with pore-to-pore distance of 12.9 nm. For higher TMB amounts the system goes through a systematic structural transition with an increase of the pore-to-pore distance to 22.6 nm. However, the overall broader scattering peaks for these samples indicate relatively less ordered structures compared to the limonene samples. The scattering peaks for the expander-rich samples (TMB-36, TMB-56 and TMB-76) have a positional ratio of 1 : √2 : √4, which implies a body centered cubic (BCC) superlattice structure. Interestingly, the patterns remain unchanged with further increase of expander amount, indicating that the pore expansion and structural transformation is complete.

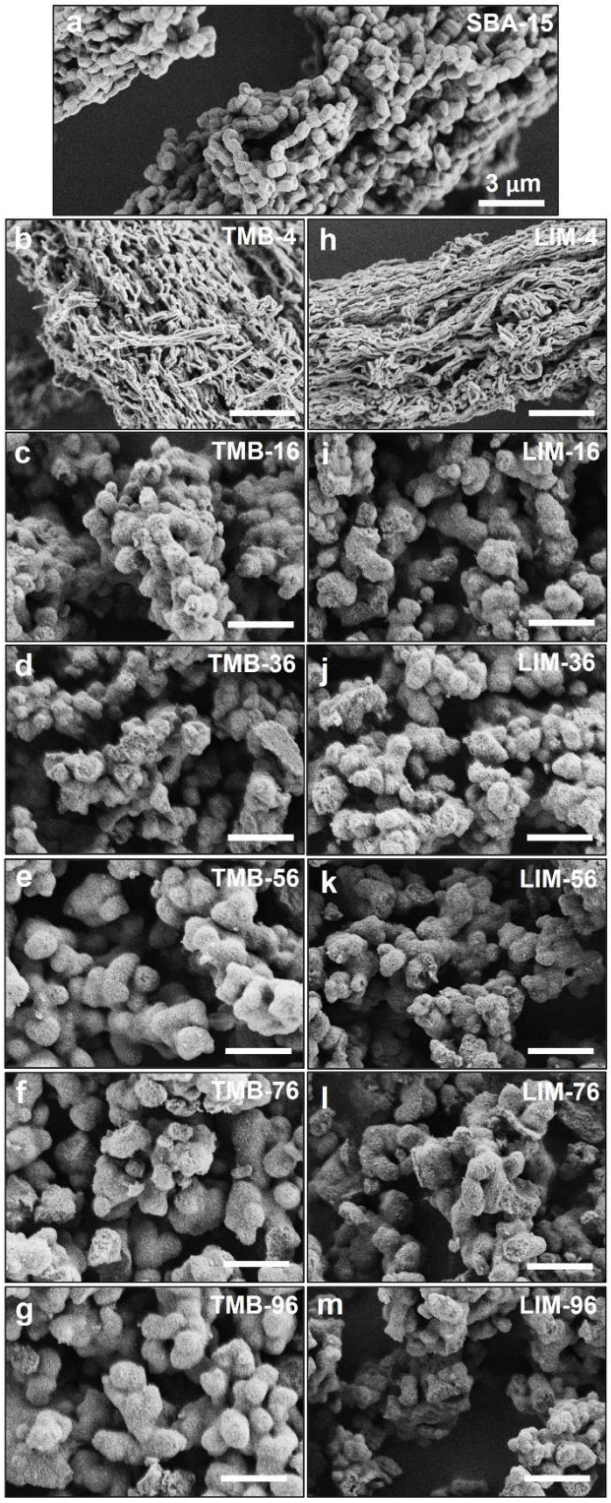

Figure 5. SEM images of SBA-15 (a) and pore expanded micellar templated silica obtained with increasing amounts of expander TMB (left column) and limonene (right column). The scale bar is 3 µm for all images.

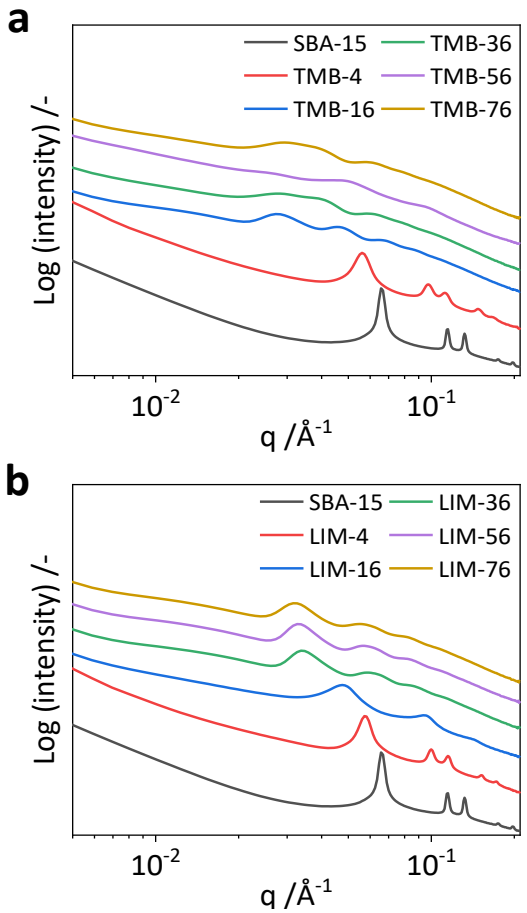

Figure 6. Small angle X-ray scattering (SAXS) patterns for mesoporous materials with various amounts of pore expanders. Sharper reflexes for SBA-15 samples shift to left and become broader with increasing amounts of expander for both, (a) TMB and (b) limonene.

Overall, the SAXS data show that both expander molecules, TMB and limonene, have similar effects on the mesopore structure formation, though the use of limonene results in a slightly more ordered pore arrangement compared to TMB under the synthesis conditions used in our experiments.

Table 1. Textural data for samples obtained with different amounts of the expanders, limonene (LIM) and TMB, respectively.

Sample	Pore size* (nm)	Specific Surface area ($m^2\ g^{-1}$)	Total pore volume ($cm^3\ g^{-1}$)
SBA-15	7.5	625	1.0
TMB-4	10.5	618	1.4
TMB-16	12.2	666	1.7
TMB-36	19.3	603	2.4
TMB-56	20.0	594	2.6
TMB-76	19.3	482	2.1
TMB-96	19.9	532	2.4
LIM-4	10.2	528	1.5
LIM-16	15.5	542	1.7
LIM-36	17.5	609	2.4
LIM-56	18.0	570	2.4
LIM-76	18.5	590	2.5
LIM-76	18.5	590	2.5

* Mode pore diameter determined from the maximum of the pore size distribution curve.

Life cycle assessment

A life cycle assessment (LCA) was performed to identify which of the two expander molecules is greener: petrochemical-based 1,3,5-trimethyl benzene (TMB, mesitylene) or limonene produced as by-product of the orange juice production. The LCA was conducted in four steps according to DIN 14040/14044: goal and scope definition, inventory analysis, impact assessment and interpretation.[42,43]

Goal and scope definition

In the first part of this contribtuion it was shown that a similar mole fraction of bio-based expander molecule limonene is required to substitute TMB in order to obtain a pore-expanded silica material with comparable properties. On this basis the functional unit for the LCA was chosen to be the production of 1 t of expander molecule for both, TMB and limonene. The cut-off-criterion was set at in-/outputs less than 1.5 wt%.

The system boundary is cradle-to-gate, i.e., from raw materials sourcing until the produced expander molecule (Figure 7). However, for the production of limonene two different allocation scenarios were chosen to deal with the ‘waste’ status of the orange peels.[44]

In scenario a) the orange peels are considered left-over waste from orange juice production as it is currently the case. Therefore, the impacts of orange tree cultivation, harvesting and orange fruit processing are solely allocated to the orange juice production. In scenario b) we assume the (bio-based economy) case that limonene (and other organic molecules) production from orange peels establishes as an economic factor of orange fruit processing. In this case the orange trees are not only harvested for orange juice production but also for the production of limonene and other valuable organic products like molasses, which justifies that at least 5 % (equal to the weight portion of limonene among the other valuable organic components in the organic fraction of orange peels of oranges) of the environmental impacts for cultivation, harvesting and orange fruit processing are allocated to the orange peel production from which limonene is extracted.

The greenness evaluation is based on the calculation of the midpoint indicators fossil resource scarcity potential, freshwater eutrophication potential, global warming potential, human carcinogenic toxicity potential, land use potential, terrestrial acidification potential and water consumption (depletion) potential.

Inventory analysis

In Figure 7 the process steps for the production of TMB and limonene from their respective raw materials as well as the system boundaries for the mass and energy balance are visualised.

TMB is produced via self-condensation of acetone.[45] The production process was not available in the ecoinvent database. Therefore we simulated this process using the AspenPlus NRTL model to estimate the respective energy input based on the literature data[45] for 80 % conversion, 70 % selectivity to TMB, a reaction temperature of 350 °C, pressure of 1 bar and a Niobium on silica catalyst (2 wt% of the reaction mixture), which has to be regenerated after 150 h time on stream through calcination at 550 °C for 18 h.[45] In addition to TMB, by-products such as mesitylene oxide, isobutene, acetic acid, C10 and C12 cyclic hydrocarbons are produced, which are valuable products. Therefore, the impacts of the self-condensation process have been allocated also to these by-products according to the selectivity (20 % by-products).

Acetone is industrially obtained as by-product of the cumene process (Hock process), where benzene and propene react to form cumene, which is then oxidised with air to cumene hydroperoxide, which is finally split into phenol and acetone.[46,47] Together with each kg of phenol 0.63 kg of acetone are produced.[48] Data about this process were already available in the ecoinvent database. The energy and mass inputs and the respective environmental impacts of the cumene process are partially allocated to phenol according to its produced fraction. Therefore, phenol is not included in the calculation of the environmental impacts of acetone production and also not included in the product system. Propene stems from crude oil processing, benzene from crude oil and coal, which was also available in the ecoinvent database.

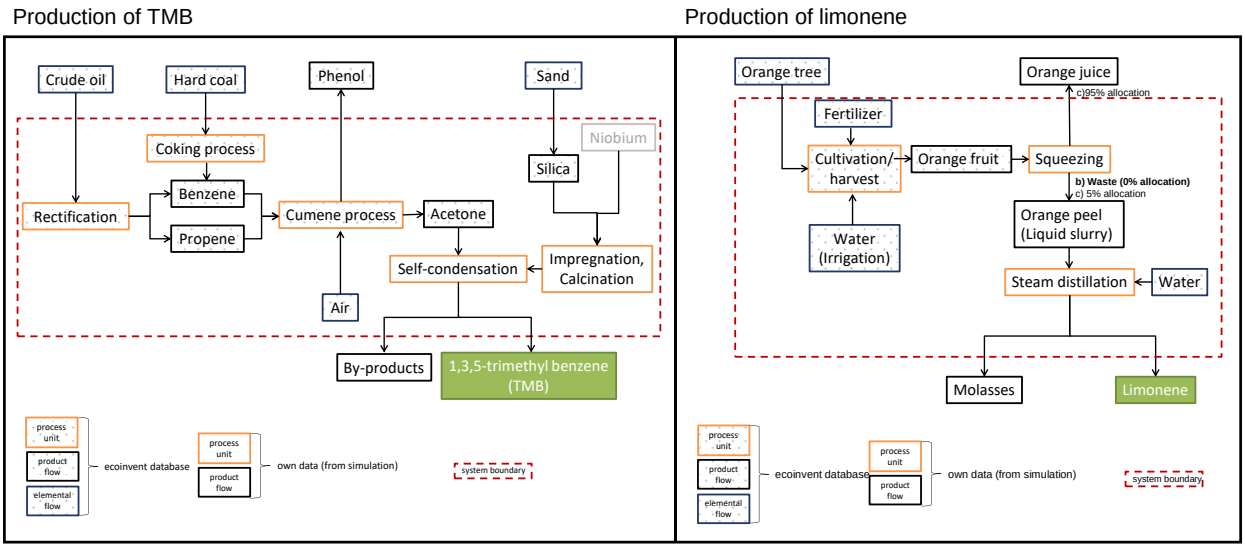

Figure 7. Process flow charts and LCA system boundaries for the production of TMB and limonene. For limonene two allocation scenarios are considered: a) the orange peels are left-over waste from orange juice production without allocation of the environmental impacts of the pre-processes to the orange peels b) the orange peels are considered a resource and accordingly the orange trees are not only harvested for orange juice production but also for the production of limonene and molasses, therefore 5 % of the environmental impacts of cultivation, harvesting and orange fruit processing are allocated to the orange peel production from which limonene is extracted.

For limonene we assessed the industrial production process from orange peels, which is currently (scenario a)) a waste product of the orange juice production.[49,50] Squeezing of oranges yields around 60 wt% juice. The remaining 40 wt% is wet orange/citrus processing waste, which consists mainly of orange peel including the segment membranes.[51] The major components of this waste are 80 wt% water, 6 wt% soluble sugars, 5 wt% cellulose and hemicellulose, 4 wt% pectin and 0.8 wt% limonene.[50,52] To isolate the limonene, steam distillation is the industrially applied process which recovers around 65 wt% of the limonene in the orange peel waste with a purity of 95%.[49,53] From these data it was calculated that around 192 t of orange peel are needed for the production of 1 t limonene (see Figure 8). The organic residues remaining as bottom product after the steam distillation contain other valuable products like molasses which can be further processed to e.g. compounds for perfumes[49,50] and bioethanol[53] for which we assume a yield of 20 t together with each tonne of limonene, which led to the 5 % allocation for limonene in scenario b.

Table 2. Allocated energy demands of the process units for the production of 1 t TMB and limonene.

Process unit	Product	Allocated energy demand/ MJ
Production of TMB		
Coking process	Benzene	2455
Rectification	Benzene	44
	Propene	678
Cumene process	Cumene (1st stage)	27071
	Acetone (2nd stage)	27093
Self-condensation	TMB	25163
Catalyst preparation and regeneration	Nb@ZSM-5	11
Production of limonene		
Orange plantation	Orange fruit	38876
Squeezing	Orange peel	20387
Steam distillation	Limonene	35944

Data for the harvesting of oranges in Spain were available in the ecoinvent database. Data for the production of orange juice yielding orange peels as a by-product were obtained from literature.[43,49,50] Only the data for steam distillation of the orange peels for the production of limonene had to be simulated to obtain the energy requirements based on process parameters given in the literature.[49,50,54] The reaction parameters and the process flow sheets of both simulated processes (TMB production via acetone self-condensation; limonene production via steam distillation of orange peels) can be found in the supplementary information in Tables S2, S3 and Figures S3, S4.

As can be seen from the inventory data in Figure 8, the cradle-to-gate production of 1 t TMB (via acetone self-condensation starting from crude oil and hard coal as visualised in Figure 7) requires a total energy of about 82523 MJ. Table 2 details the respective energy contributions of the different process units which are allocated to the production chain of TMB withing the LCA system boundaries. From there it can be seen that the largest contributors to the energy consumption of TMB production are the acetone self-condensation process (25163 MJ = 30 % of the total energy demand) and the Cumene process (27071 MJ + 27093 MJ = 66 % of the total energy demand).

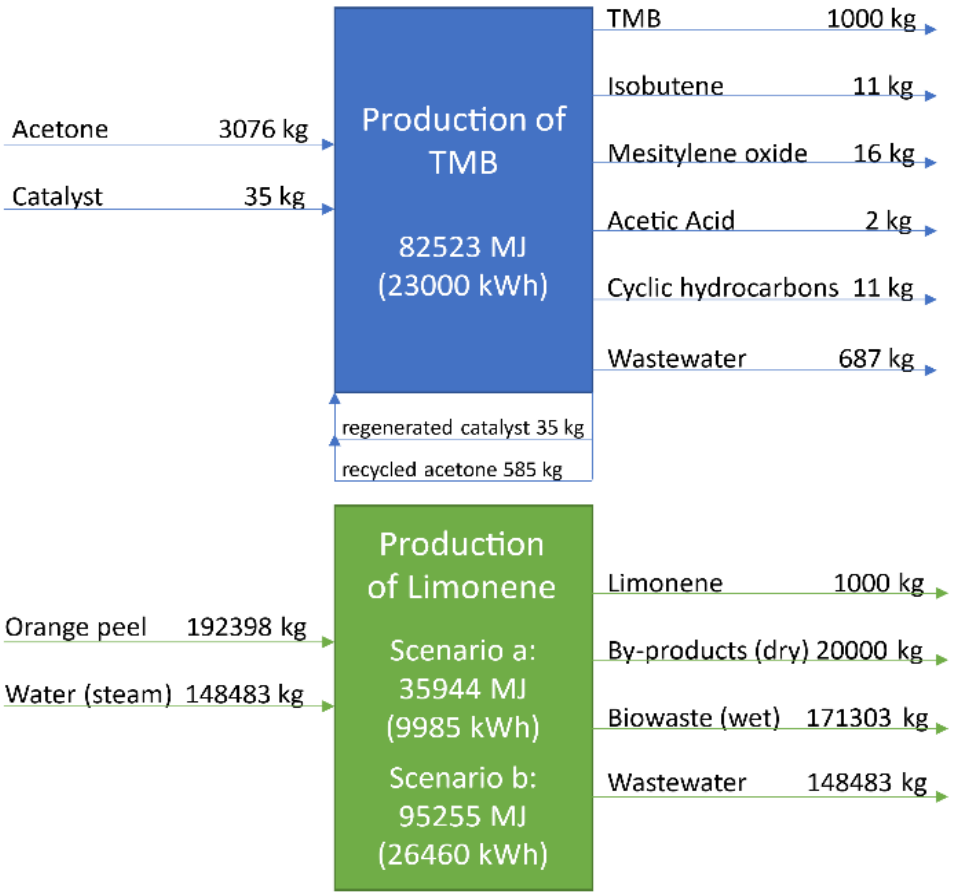

Figure 8. Life cycle inventory: Mass inputs and outputs and total allocated energy consumption for the cradle-to-gate production of TMB via self-condensation of acetone and production of limonene via steam distillation of orange peels, which are treated as waste (scenario a) or chemical resource with 5 % of the impacts for orange tree harvesting and fruit processing allocated to the orange peels.

If the pre-processes for the orange peels are not allocated to limonene (waste scenario a) then the cradle-to-gate production of 1 t limonene counts only the energy for the steam distillation of the orange peels, i.e. 35944 MJ, which is less than half of the energy demand for TMB production. If the orange peel pre-processes are allocated with 5 % to limonene (value product scenario b) then 5 % of the energy consumption of orange tree plantation and harvesting, i.e. 38876 MJ, and 5 % of the energy consumption of the orange fruit squeezing process, i.e. 20387 MJ, have to be added to the steam distillation demand, leading to a total cradle-to-gate energy requirement of 95255 MJ, which is 15 % more than the energy required for TMB production.

Furthermore, Figure 8 details the output streams of the production of TMB and limonene, respectively. Acetone reacts via self-condensation to form TMB. The unconverted acetone (25 %) is recycled back into the process. Around 5 wt% of the output are by-products like cyclic hydrocarbons, acetic acid, mesityl oxide und isobutene. Since these are value products, 5 % of the process impacts are allocated to them and not to TMB.

Impact assessment and interpretation

In general, if a chemical is called “greener” it should have less environmental impacts compared to its conventional counterpart. To assess such potential environmental impacts quantitatively, several impact categories have been defined with their respective indicators which are calculated from the outputs of the mass and energy balances obtained in the inventory analysis of the life cycle assessment.

Accordingly in our case an expander molecule and the MCF synthesis using this expander molecule (if all other synthesis parameters are kept constant and similar use and end-of-life phases are assumed) would be greener if its potential impact on e.g., fossil resource depletion, global warming, water pollution and human health is less. Therefore, in this impact assessment we determined the following potential environmental impacts: fossil resource scarcity (FRS, indicator unit kg oil eq.), freshwater eutrophication potential (FWE, indicator unit kg 1,4-DCB eq.), global warming potential (GWP, unit kg CO2 eq.), land use (unit m^2a crop eq.), human carcinogenic toxicity (HTP, unit kg 1,4-DCB eq.), terrestrial acidification (TAP, unit kg SO2 eq.) and water depletion potential (WDP, unit m^3).

As can be seen in the left spider chart in Figure 9, limonene (green curve) has much lower environmental impacts than TMB if it is produced from orange peel waste. The significant contributions of limonene production to freshwater eutrophication, global warming and human carcinogenic toxicity stem solely from use of the conventional energy mix (containing 50 % coal, gas, oil and radioactive sources) because they disappear completely if the energy mix is changed to 100 % renewable (Figure 9, top right).

In a future bioeconomy, where limonene might become a more important chemical whose demand exceeds the generation of orange (citrus) peel waste and might lead to the plantation and harvesting of orange fruit not only for juice but also for limonene production, the allocation scenario b (5 % allocation of the pre-process impacts to limonene production) will be of relevance. In this case, using the conventional energy mix, limonene production shows worse effects in almost all impact categories compared to TMB, except for fossil resource scarcity and global warming potential. Looking at the process contributions for limonene in Figure 9 (bottom right) the reason for this worse effect is the high amount of energy required for the steam distillation step. Here, we assumed the current German electricity mix, of which only 50 % is renewable energy.[55] Also the current energy sources used in Spain for growing and processing oranges are mostly oil and coal power-based, which strongly influences environmental impacts such as freshwater eutrophication potential, global warming potential and human carcinogenic toxicity.[55] The high land use and water consumption is caused by the cultivation of the orange tree plantations. Since the content of limonene in orange (citrus) peels is pretty small (see Figure 8), a huge amount of orange trees has to be cultivated to yield 1 t of limonene.

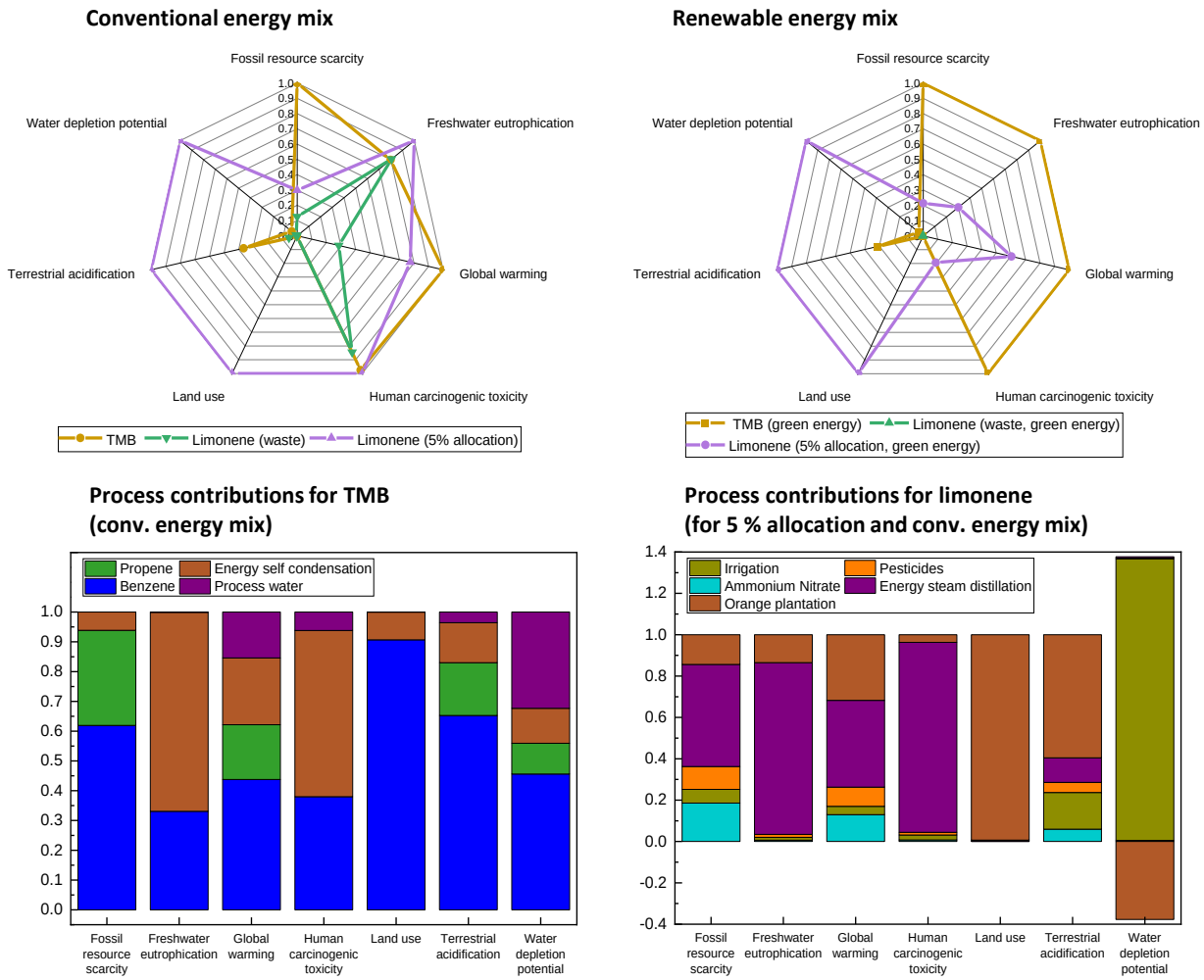

Figure 9. Spider charts comparing the allocated potential environmental impacts of the production of the two expander molecules using the conventional energy mix (top left) and using 100 % renewable energy for the gate-to-gate production part (top right); bottom: detailed bar charts for the relative process contributions to the environmental impacts for the cradle-to-gate production using the conventional energy mix for TMB (left) and limonene (right, scenario b with 5 % allocation).

In the production of TMB, the intermediate benzene production (67 % from crude oil processing, 33 % from coal coking) has a strong influence on all environmental impacts except water consumption. Propene, on the other hand, which is mainly produced via steam cracking of longer-chain alkanes (C5-C10) or naphtha, has much less influence on the potentials compared to benzene production (Figure 9 bottom left).

To show how a (future) fossil-free energy mix of 100 % renewable energy sources (composed of 95 % hydro power, 2 % wind power, 3 % biomass) would influence the environmental impacts of TMB and limonene production, we added the spider chart for the scenario '100 % renewable energy' in Figure 9 (top right). It can be seen that the potential impacts of limonene production (scenario with 5 % allocation) on fossil resource scarcity, freshwater eutrophication, global warming and human carcinogenic toxicity are significantly reduced if the energy demand (which is especially high for the steam distillation step) is covered by this 100 % renewable energy mix.

However, independent of the energy mix, in scenario b the potential impacts of limonene production on land use, acidification potential (due to fertiliser use) as well as water consumption (for irrigation) are always higher compared to TMB. This stems primarily from the orange tree plantation. In general, it is very typical for chemicals from renewable sources that their production impacts those three impact categories much more compared to fossil-based chemicals where no trees or plants have to be grown and it will be the task of future (sustainable)

farming systems to reduce those impacts as much as possible, especially if also an increased amount of chemicals is to be produced in this way.

For the current scenario (a), where the orange peels are still a waste product of the food industry, the environmental impacts of limonene production using 100 % renewable energy are remarkably low and close to neutral. Accordingly, the claim of limonene being a greener expander molecule than TMB (and many other fossil-based molecules) for the preparation of porous materials is very valid at the moment but bound to the precondition that it is produced from citrus peel waste and not from citrus fruit, which is purposefully grown also for the production of limonene. Otherwise, limonene will only be greener than TMB in terms of fossil resource scarcity potential, global warming potential and (if 100 % renewable non-biogenic energy sources are used for its production) also human carcinogenic toxicity and freshwater eutrophication potential.

The cultivation and irrigation of oranges and other citrus fruit has a high impact on terrestrial acidification. With better irrigation systems and a change to ecological/sustainable agriculture instead of monocultures, which avoid the consumption of artificial fertilizers and pesticides and enable and intensive irrigation, the environmental impacts of limonene-based applications will be further reduced. However, if in future the demand of limonene exceeds the generated amount of citrus peel waste, then also other sources for limonene production (e.g. turpentine oil) and the use of alternative renewable molecules have to be considered on the basis of further comparative life cycle assessments to avoid over-burdening of the natural environment with process-related impacts.[56]

Conclusions

Pore-expanded micellar templated silica materials were synthesised using limonene as a renewable alternative for the conventionally applied pore expander trimethylbenzene (TMB) and the effect of both expander molecules on the resulting material properties was compared. Nitrogen physisorption analysis showed that the same amount of limonene is needed to successfully expand the pore size from 7.5 nm (without expander) up to the largest possible extent of 17-19 nm (19-20 nm for TMB). TEM and SEM analyses indicated similar pore and particle morphologies obtained with limonene and TMB, respectively. Together with SAXS analysis a slight difference between the action of TMB and limonene was found in the maintenance of an ordered pore structure up to an expander/P123 molar ratio of 16 for limonene, while with TMB the structural loss was already more pronounced at this expander amount. However, at a ratio of 36 the transformation towards disordered pore structure with maximum pore diameter was complete for both expanders, TMB and limonene, which demonstrates that limonene is a versatile substitute for fossil-based TMB because it can fully overtake its function as a pore expander.

With a cradle-to-gate life cycle assessment (LCA) for both expander molecules we could prove that limonene is indeed a very green substitute for TMB if it is produced from citrus/orange peel waste, especially if a 100 % renewable energy mix is used, which is generally very desirable for a sustainable development (UN SDGs 7 and 13).

After showing that limonene is a greener alternative to TMB for pore expanding purposes, we hope to stimulate further exploration of this and other renewable organic molecule for greener syntheses of porous materials and their application, which would be a valid contribution to a more sustainable materials basis of our society (UN SDG 12).

Experimental Section

Materials

Hydrochloric acid (HCl, 37%, VWR), Pluronic P123 (P123, 5800 g mol^{-1}, Sigma-Aldrich), 1,3,5-trimethylbenzene (TMB, ≥98.5%, Thermo Scientific), Limonene (≥95%, D and L type mixture, Sigma-Aldrich), ammonium fluoride (NH_4F, 98%, Sigma-Aldrich), tetraethyl-orthosilicate (TEOS, ≥99 %, GPR RECTAPUR®, VWR) and sodium hydroxide (NaOH, ≥98 %, in pellets, VWR) were all used as received. De-ionized water was used for all synthesis and cleaning procedures. All reaction vessels were cleaned using 5 wt% aqueous NaOH solution, before use.

Synthesis of SBA-15 and pore-expanded micellar templated silica

In a typical procedure, 20.55 g of water and 4.93 g of hydrochloric acid were mixed and 0.83 g of P123 was added to it at room temperature. The solution was stirred at 500 rpm in a 60 ml polypropylene (PP) bottle with a circular cross-section of 4 cm containing an elliptical magnetic stirring bar (32 mm x 15 mm). The reaction vessel was kept closed by a screw cap and was only opened when adding further reactants. Then the necessary amount of micelle expander (0.07 g for sample TMB-4, 0.3 g for TMB-16, 0.6 g for TMB-36, 1 g for TMB-56, 1.3 g for TMB-76, 1.3 g for TMB-96, 0.08 g for LIM-4, 0.3 g for LIM-16, 0.7 g for LIM-36, 1.1 g for LIM-56, 1.5 g for LIM-76, 1.9 g for LIM-96) and 0.01 g of NH4F was added. After stirring for 1 h, 1.75 g of TEOS was added. The molar ratios used for all the samples are listed in Table 3. After 1 h of further stirring, the reaction vessel (PP bottle) was placed in a circulating oven at 40 °C for 20 h. Afterwards, the solution was transferred to a 45 mL polytetrafluoroethylene (PTFE) lined autoclave (Parr). The autoclave was then placed in the circulating oven at 100 °C for 24 h. Afterwards, the autoclave was allowed to cool down. Its contents were then centrifuged (6500 rpm for 5 min) and the sedimented material was washed 2 times with ethanol and one time with water. The obtained material was then dried at 75 °C overnight. The dried sample was then crushed in a mortar and transferred to a heat-resistant ceramic crucible. The crucible was placed inside a calcination furnace and heated to 550 °C with a ramp of 2 °C min^{-1}, under an airflow of 50 L h^{-1}, for 6 h to remove any organic residues. After calcination, the sample was again crushed with a mortar and transferred to a sample container.

Table 3. Names and molar ratios of chemicals used for all the synthesized samples.

Sample	P123	Expander	TEOS	HCl	H2O	NH_4F
SBA-15	1	0	59	350	9200	2
TMB-4	1	4	59	350	9200	2
TMB-16	1	16	59	350	9200	2
TMB-36	1	36	59	350	9200	2
TMB-56	1	56	59	350	9200	2
TMB-76	1	76	59	350	9200	2
TMB-96	1	96	59	350	9200	2
LIM-4	1	4	59	350	9200	2
LIM-16	1	16	59	350	9200	2
LIM-36	1	36	59	350	9200	2
LIM-56	1	56	59	350	9200	2
LIM-76	1	76	59	350	9200	2
LIM-96	1	96	59	350	9200	2

Nitrogen physisorption

All the samples were degassed prior to measurements using a vacuum degasser (MasterPrep Degasser, Quantachrome Instruments) at 250°C for 12 hours. The nitrogen physisorption measurements were conducted using Quadrasorb (Quantachrome Instruments) at 77 K. The specific surface area was calculated using Brunauer, Emmett and Teller (BET) method in the relative pressure range from 0.05 to 0.36 and the micropore volume was determined using the t-plot in the range from 0.3 to 0.5 p/p_0. The pore size distributions were calculated using the non-linear density function theory (NLDFT) model for cylindrical pores from the adsorption and desorption branches of the isotherms.

SEM

The SEM analysis was conducted via GeminiSEM 500 (Zeiss) using a secondary electron detector. The measurements were performed at 1 kV voltage with an aperture size of 15 µm.

TEM

The TEM analysis was carried out in high-angle annular dark-field scanning transmission electron microscopy (HAADF-STEM) mode using a Titan Themis^3 300 transmission electron microscope (Thermo Fisher Scientific). The images were acquired at 300 kV.

SAXS

SAXS measurements were carried out with an in-house SAXS setup (VAXSTER; Versatile X-ray Scattering Instrument Erlangen) in transmission geometry.[57,58] It uses a 250 W liquid Gallium jet X-ray source (Excillum) providing an X-ray wavelength of 1.34 Å. The powder samples were filled in 1 mm glass capillaries and placed at the sample position inside the evacuated (~ 10^{-3} mbar) detector tube. The X-ray beam was monochromatized and focussed trough a 2.5 m collimation line with 3 double slit systems (two of which equipped with single crystal scatterless Si blades) to a beam cross section of ~ 0.36 x 0.36 mm^2 at the sample position by a 15 cm Montel optics (Incoatec). A Dectris Pilatus3 300k detector was used to record the SAXS images at a sample-to-detector distance of 1.6 m. The X-ray path was fully evacuated and each measurement was collected for 1 hour for sufficient statistics. The collected 2D isotropic SAXS pattern were azimuthally averaged and the resulting 1D scattering profiles were plotted and analysed.

Life cycle assessment (LCA)

In this study, a comparative assessment of the greenness (ecological impacts) of the two expander molecules, namely the petrochemical-based trimethylbenzene (TMB) and the bio-based limonene, was undertaken in the context of a life cycle assessment (LCA). The LCA was conducted according to DIN EN ISO 14040/44[42] with goal and scope definition, inventory analysis, impact assessment and interpretation. For the data management the LCA software openLCA (version 10.1.3) and the database ecoinvent 3.7.1 were used. Calculation method for the midpoint categories was ReCiPe 2016 Midpoint (H).[59] Energy input data which were not available in the ecoinvent database were simulated using the

programme Aspen (Version 10). The parameters used for these simulations are detailed in Table S2 in the supplementary information.

Conflicts of Interests

There are no conflicts of interest to declare.

Acknowledgement

This project was funded by the Deutsche Forschungsgemeinschaft (DFG, German Research Foundation)– Project-ID 416229255 – SFB 1411 and Project-ID 431791331 – SFB 1452. S.M. and T.U. acknowledge DFG support by NFDI 10/1 DAPHNE4NFDI. Furthermore, the authors acknowledge Marvin Gornik, Nora Elhaus and Leon Ewald for their preliminary work.

References

1 J. B. Zimmerman, P. T. Anastas, H. C. Erythropel and W. Leitner, *Science*, 2020, **367**, 397–400.
2 H. C. Erythropel, J. B. Zimmerman, T. M. de Winter, L. Petitjean, F. Melnikov, C. H. Lam, A. W. Lounsbury, K. E. Mellor, N. Z. Janković, Q. Tu, L. N. Pincus, M. M. Falinski, W. Shi, P. Coish, D. L. Plata and P. T. Anastas, *Green Chemistry*, 2018, **20**, 1929–1961.
3 J. Florek, R. Guillet-Nicolas and F. Kleitz, in *For Energy, Sustainable Development and Biomedical Sciences*, ed. M. Leclerc and R. Gauvin, De Gruyter, 2014, pp. 61–100.
4 X. Yu and C. T. Williams, *Catalysis Science & Technology*, 2022, **12**, 5765–5794.
5 C. Bonzom, L. Schild, H. Gustafsson and L. Olsson, *BMC Biochemistry*, 2018, **19**, 1.
6 I. Díaz, R. M. Blanco, M. Sánchez-Sánchez and C. Márquez-Álvarez, in ed. V. Blay, L. F. Bobadilla and A. Cabrera García, Amsterdam University Press, 2018, pp. 149–174.
7 R. Zubrzycki and T. Ressler, *Microporous and Mesoporous Materials*, 2015, **214**, 8–14.
8 N. Rahmat, A. Z. Abdullah and A. R. Mohamed, *American Journal of Applied Sciences*, 2010, **7**, 1579–1586.
9 T. M. Albayati, I. K. Salih and H. F. Alazzawi, *Heliyon*, 2019, **5**, e02539.
10 A.-M. Putz, A. Policicchio, S. Stelitano, P. Sfîrloagă, C. Ianăşi, R. G. Agostino and S. Cecilia, *Fullerenes, Nanotubes and Carbon Nanostructures*, 2018, **26**, 810–819.
11 R. Guillet-Nicolas, F. Bérubé, M. Thommes, M. T. Janicke and F. Kleitz, *The Journal of Physical Chemistry C*, 2017, **121**, 24505–24526.
12 J. S. Lettow, Y. J. Han, P. Schmidt-Winkel, P. Yang, D. Zhao, G. D. Stucky and J. Y. Ying, *Langmuir*, 2000, **16**, 8291–8295.
13 P. Schmidt-Winkel, Lukens,, Wayne W., P. Yang, D. I. Margolese, J. S. Lettow, J. Y. Ying and G. D. Stucky, *Chemistry of Materials*, 2000, **12**, 686–696.
14 D. Desplantier-Giscard, A. Galarneau, F. Di Renzo and F. Fajula, in *Studies in Surface Science and Catalysis : Zeolites and Mesoporous Materials at the dawn of the 21st century*, ed. A. Galarneau, F. Fajula, F. Di Renzo and J. Vedrine, Elsevier, 2001, vol. 135, p. 205.
15 O. Daoura, S. Daher, M.-N. Kaydouh, N. El Hassan, P. Massiani, F. Launay and M. Boutros, *International Journal of Hydrogen Energy*, 2018, **43**, 17205–17215.
16 P.-C. Kuo, Z.-X. Lin, T.-Y. Wu, C.-H. Hsu, H.-P. Lin and T.-S. Wu, *RSC Advances*, 2021, **11**, 10010–10017.
17 L. Huang and M. Kruk, *Chemistry of Materials*, 2015, **27**, 679–689.
18 M. Kruk, *Accounts of Chemical Research*, 2012, **45**, 1678–1687.
19 Y. Awoke, Y. Chebude and I. Díaz, *Molecules*, 2020, **25**.
20 C. Gérardin, J. Reboul, M. Bonne and B. Lebeau, *Chemical Society Reviews*, 2013, **42**, 4217–4255.
21 A. Galarneau, F. Sartori, M. Cangiotti, T. Mineva, F. Di Renzo and M. F. Ottaviani, *The Journal of Physical Chemistry B*, 2010, **114**, 2140–2152.
22 A. G. Kong, H. W. Wang, Z. He, H. M. Ding and Y. K. Shan, *Materials Letters*, 2008, **62**, 2973–2976.

23 P. Botella, A. Corma and M. Quesada, *Journal of Materials Chemistry*, 2012, **22**, 6394–6401.
24 Z. Moradi and A. Ghorbani-Choghamarani, *RSC Advances*, 2023, **13**, 2265–2268.
25 Z. Gao and I. Zharov, *Chemistry of Materials*, 2014, **26**, 2030–2037.
26 C. P. Canlas and T. J. Pinnavaia, *RSC Advances*, 2012, **2**, 7449–7455.
27 M. Ulfa, D. Prasetyoko, W. Trisunaryanti, H. Bahruji, Z. A. Fadila and N. A. Sholeha, *Scientific Reports*, 2022, **12**, 15271.
28 N. Baccile, N. Nassif, L. Malfatti, I. N. A. van Bogaert, W. Soetaert, G. Pehau-Arnaudet and F. Babonneau, *Green Chemistry*, 2010, **12**, 1564–1567.
29 G. Feng, J. Wang, M. Boronat, Y. Li, J.-H. Su, J. Huang, Y. Ma and J. Yu, *Journal of the American Chemical Society*, 2018, **140**, 4770–4773.
30 M. Virot, V. Tomao, C. Ginies, F. Visinoni and F. Chemat, *Journal of Chromatography A*, 2008, **1196-1197**, 147–152.
31 M. A. Martin-Luengo, M. Yates, E. S. Rojo, D. Huerta Arribas, D. Aguilar and E. Ruiz Hitzky, *Applied Catalysis A: General*, 2010, **387**, 141–146.
32 P. Bajpai, in *Biermann's Handbook of Pulp and Paper (Third Edition)*, ed. P. Bajpai, Elsevier, 2018, pp. 363–371.
33 European Chemicals Agency, *Candidate list of substances of very high concern for authorisation,* available at: https://echa.europa.eu/candidate-list-table, accessed January 2023.
34 B. W. Brooks, *Green Chemistry*, 2019, **21**, 2575–2582.
35 P. T. Anastas and J. C. Warner, *Green chemistry: theory and practice*, Oxford University Press, New York, 1998.
36 M. Thommes, K. Kaneko, A. V. Neimark, J. P. Olivier, F. Rodriguez-Reinoso, J. Rouquerol and K. S. Sing, *Pure and Applied Chemistry*, 2015, **87**, 1051–1069.
37 C. Schlumberger and M. Thommes, *Advanced Materials Interfaces*, 2021, **8**, 2002181.
38 M. Thommes, B. Smarsly, M. Groenewolt, P. I. Ravikovitch and A. V. Neimark, *Langmuir*, 2006, **22**, 756–764.
39 H. I. Lee, J. H. Kim, G. D. Stucky, Y. Shi, C. Pak and J. M. Kim, *Journal of Materials Chemistry*, 2010, **20**, 8483–8487.
40 S. Maiti, A. André, S. Maiti, M. Hodas, M. Jankowski, M. Scheele and F. Schreiber, *The Journal of Physical Chemistry Letters*, 2019, **10**, 6324–6330.
41 M. Kruk, M. Jaroniec, C. H. Ko and R. Ryoo, *Chemistry of Materials*, 2000, **12**, 1961–1968.
42 UNE EN ISO 14044:2006/A1:2018, *Environmental management - Life cycle assessment - Requirements and guidlines*, Beuth, 2018.
43 ESU-services Ltd., *Life cycle assessment of orange juice Harmonised Environmental Sustainability in the European food and drink chain,* available at: https://esu-services.ch/fileadmin/download/doublet-2013-SENSE_Deliverable-2_1-LCAorangejuice.pdf.
44 R. Heijungs and J. B. Guinée, *Waste Management*, 2007, **27**, 997–1005.
45 *United States Pat.*, US 7,157,397 B2, 2004.
46 V. M. Zakoshansky, *Petroleum Chemistry*, 2007, **47**, 273–284.
47 B. G. Walter Klöpffer, *Life Cycle Assessment (LCA): A Guide to Best Practice*, John Wiley & Sons, Ltd, 2014.
48 Martin Gallardo Hipolito, *Life Cycle Assessment of platform chemicals from fossil and lignocellulosic biomass scenarios: phenolic compounds, solvent, soft and hard platic precursors*, Lambert Academic Publishing, 2011.
49 R. Ciriminna, M. Lomeli-Rodriguez, P. Demma Carà, J. A. Lopez-Sanchez and M. Pagliaro, *Chemical Communications*, 2014, **50**, 15288–15296.
50 W. Widmer, W. Zhou and K. Grohmann, *Bioresource Technology*, 2010, **101**, 5242–5249.
51 M. Pourbafrani, G. Forgács, I. S. Horváth, C. Niklasson and M. J. Taherzadeh, *Bioresource Technology*, 2010, **101**, 4246–4250.
52 K. Grohmann, R. G. Cameron and B. S. Buslig, *Bioresource Technology*, 1995, **54**, 129–141.
53 Weiyang Zhou, Wilbur W. Widmer and Karel Grohmann, in 2007.
54 I. John, K. Muthukumar and A. Arunagiri, *International Journal of Green Energy*, 2017, **14**, 599–612.
55 International Energy Agency, *World Energy Balances,* available at: https://www.iea.org/data-and-statistics/data-product/world-energy-balances.
56 S. A. Matlin, S. E. Cornell, A. Krief, H. Hopf and G. Mehta, *Chemical Science*, 2022, **13**, 11710–11720.
57 I. Schuldes, D. M. Noll, T. Schindler, T. Zech, K. Götz, M.-S. Appavou, P. Boesecke, F. Steiniger, P. S. Schulz and T. Unruh, *Langmuir*, 2019, **35**, 13578–13587.
58 T. Kassar, N. S. Güldal, M. Berlinghof, T. Ameri, A. Kratzer, B. C. Schroeder, G. L. Destri, A. Hirsch, M. Heeney, I. McCulloch, C. J. Brabec and T. Unruh, *Advanded Energy Materials*, 2016, **6**, 1502025.
59 M. A. J. Huijbregts, Z. J. N. Steinmann, P. M. F. Elshout, G. Stam, F. Verones, M. Vieira, M. Zijp, A. Hollander and R. van Zelm, *The International Journal of Life Cycle Assessment*, 2017, **22**, 138–147.